

IMEX finite volume methods for cloud simulation

M. Lukáčová-Medvidová, J. Rosemeier, P. Spichtinger and B. Wiebe

Abstract We present new implicit-explicit (IMEX) finite volume schemes for numerical simulation of cloud dynamics. We use weakly compressible equations to describe fluid dynamics and a system of advection-diffusion-reaction equations to model cloud dynamics. In order to efficiently resolve slow dynamics we split the whole nonlinear system in a stiff linear part governing the acoustic and gravitational waves as well as diffusive effects and a non-stiff nonlinear part that models nonlinear advection effects. We use a stiffly accurate second order IMEX scheme for time discretization to approximate the stiff linear operator implicitly and the non-stiff nonlinear operator explicitly. Fast microscale cloud physics is approximated by small scale subiterations.

Key words: weakly compressible flows, Euler equations, Navier-Stokes equations, low Mach number, IMEX schemes, cloud physics, multiphase system

MSC (2010): 65M08, 65N08, 35Q30, 35L65

M. Lukáčová-Medvidová
Institute of Mathematics, Johannes Gutenberg-University Mainz
Staudingerweg 9, 55 128 Mainz, Germany
e-mail: lukacova@uni-mainz.de

J. Rosemeier
Institute of Atmospheric Physics, Johannes Gutenberg-University Mainz
Becherweg 21, 55 128 Mainz, Germany
e-mail: rosemeie@uni-mainz.de

P. Spichtinger
Institute of Atmospheric Physics, Johannes Gutenberg-University Mainz
Becherweg 21, 55 128 Mainz, Germany
e-mail: spichtin@uni-mainz.de

B. Wiebe
Institute of Mathematics, Johannes Gutenberg-University Mainz
Staudingerweg 9, 55 128 Mainz, Germany
e-mail: b.wiebe@uni-mainz.de

1 Mathematical model

In this paper we present a new operator splitting finite volume method for weakly compressible flows including cloud dynamics. The mathematical model consists of the Navier-Stokes equations describing weakly compressible fluid flow including viscous and friction effects. Further atmospheric factors like the Coriolis force and turbulence are not considered in this paper. In order to model microscale cloud physics we add evolution equations for water vapor, cloud water and rain. Phase change between these phases is modeled by an advection-diffusion-reaction system. Note that the total mass of the dry air remains constant, whereas the momentum and energy are not conserved, but satisfy the balance laws.

Let \bar{p} , $\bar{\rho}$, $\bar{\mathbf{u}} (= 0)$, $\bar{\theta}$, $\bar{\rho}\bar{\theta}$ express the pressure, density, velocity, potential temperature and energy for a dry background state, which is in the hydrostatic equilibrium

$$\partial_{x_3}\bar{p} = -\bar{\rho}g,$$

where $g = 9.81[m/s^2]$ is the gravitational acceleration. Furthermore let p' , ρ' , \mathbf{u}' , θ' , $(\rho\theta)'$ stand for the corresponding perturbations of the background states. Thus, we have $p = \bar{p} + p'$, $\rho = \bar{\rho} + \rho'$, $\theta = \bar{\theta} + \theta'$, and $(\rho\theta) = \bar{\rho}\bar{\theta} + \bar{\rho}\theta' + \rho'\bar{\theta} + \rho'\theta' \equiv \bar{\rho}\bar{\theta} + (\rho\theta)'$. Since the background velocity $\bar{\mathbf{u}} = 0$, it holds $\mathbf{u} \equiv \mathbf{u}'$ and we will omit the prime symbol hereinafter.

In order to avoid numerical instabilities due to the multiscale flow behavior in the case of low Mach number limit, numerical simulations are typically realized for the perturbations, which satisfy the following equations

$$\begin{aligned} \partial_t \rho' + \nabla \cdot (\rho \mathbf{u}) &= 0, \\ \partial_t (\rho \mathbf{u}) + \nabla \cdot (\rho \mathbf{u} \otimes \mathbf{u} + p' \text{Id} - \rho \mu_m (\nabla \mathbf{u} + (\nabla \mathbf{u})^T)) &= -\rho' g \mathbf{e}_3 \equiv -\rho' g \begin{pmatrix} 0 \\ 0 \\ 1 \end{pmatrix}, \\ \partial_t (\rho \theta)' + \nabla \cdot (\rho \theta \mathbf{u} - \rho \mu_h \nabla \theta) &= S_\theta, \end{aligned} \quad (1)$$

where μ_m, μ_h are viscosity and heat conductivity constants. To include the moist dynamics we use in $(1)_3$ instead of the potential temperature for dry air the moist potential temperature. Denoting T the temperature, the moist potential temperature can be approximated as

$$\theta = \frac{R_m}{R} T \left(\frac{p_0}{p} \right)^{R_m/c_p},$$

where $p_0 = 10^5 [Pa]$ is the reference pressure, $R = 287.05 [J/(kg \cdot K)]$ is the gas constant of dry air, $R_m = (1 - q_v - q_c - q_r)R + q_v R_v$ is the modified gas constant of moist air and $c_p = 1005 [J/(kg \cdot K)]$, $R_v = 461.51 [J/(kg \cdot K)]$. The mass fractions of water vapor, cloud water and rain are denoted by q_v , q_c and q_r , respectively; their evolution equations will be specified below, cf. (2).

In order to close the system we determine pressure from the state equation including moisture $p = p_0 \left(\frac{R\rho\theta}{p_0} \right)^{\gamma_m}$, $\gamma_m = \frac{c_p}{c_p - R_m}$. The source term S_θ that is re-

lated to the cloud microphysics for moist processes, cf. (2), expresses the released or absorbed latent heat. For dry case R_m reduces to R and $S_\theta = 0$.

For representing (liquid) clouds in models, different approaches are described in literature, see, e.g., [4, 6] and references therein. In the present study we use a so-called single moment scheme, i.e. evolution equations for mass concentrations of water vapor q_v , cloud water q_c and rain q_r are coupled to the system of equations (1). The formulation of cloud models is not possible from first principles, since some approximations and fits to experimental data must be used in order to formulate the equations for mass concentrations only. We chose a consistent approach for modeling the process rates in the cloud model, combining existing approaches in a meaningful way, see, e.g., [9]. The microphysical cloud processes of warm clouds are modeled by the following advection-diffusion-reaction system

$$\begin{aligned}\partial_t(\rho q_v) + \nabla \cdot (\rho q_v \mathbf{u} - \rho \mu_h \nabla q_v) &= -C + E, \\ \partial_t(\rho q_c) + \nabla \cdot (\rho q_c \mathbf{u} - \rho \mu_h \nabla q_c) &= C - A_1 - A_2, \\ \partial_t(\rho q_r) + \nabla \cdot (\rho q_r \mathbf{u} - \rho v_q \mathbf{e}_3 q_r - \rho \mu_h \nabla q_r) &= A_1 + A_2 - E.\end{aligned}\quad (2)$$

The term $\nabla \cdot (-\rho v_q \mathbf{e}_3 q_r)$, where $v_q \sim q_r^{1/5}$ is the raindrop fall velocity, represents the sedimentation of rain water. C , E , A_1 , A_2 denote rates of condensation and evaporation (phase transition vapor/water) and collision rates. We assume that cloud water does not sediment by gravity, whereas rain water falls downwards. Thus, we introduce autoconversion A_1 for colliding cloud drops forming rain and accretion A_2 for rain droplets growing by collecting cloud water. Thermodynamic equilibrium is determined by saturation mixing ratio $q_* = q_*(p, T)$. Thus, the source terms can be formulated as follows:

$$C \sim q_c(q_v - q_*), \quad E \sim q_r^{1/2}(q_* - q_v), \quad A_1 \sim q_c^2, \quad A_2 \sim q_c q_r^{19/20}.$$

Note that in general cloud physics parametrisations show stiff behavior. The stiffness is a result of modeling processes with power laws containing exponents α with $0 < \alpha < 1$. To close the coupled model (1), (2) we express the potential temperature source term as

$$S_\theta = \rho \frac{L}{c_p} \frac{\theta}{T} (C - E)$$

with the specific latent heat of vaporization $L = 2.53 \cdot 10^6 [J/kg]$. Note that we formulate condensation and evaporation processes explicitly, in contrast to the usual approach of saturation adjustment, see, e.g. [7], which is commonly used in operational weather forecast models. The explicit formulation introduces additional stiff terms and very small time scales.

2 Numerical scheme

The numerical approximation of the coupled model (1), (2) is realized by the operator splitting approach. We split the whole system into the macroscopic flow equations and microscopic cloud model. The macroscopic model is approximated by the IMEX finite volume scheme. On the other hand the cloud equations are approximated using several subiterations of the same implicit-explicit scheme using smaller time steps. The macroscopic flow equations use the solution of the microscopic cloud model at the last time step and the cloud model uses the solution of the flow equations from the new time step. This yields to a first order splitting. In order to increase the accuracy the second order Strang splitting can be used.

2.1 IMEX finite volume scheme for the Navier-Stokes equations

In order to take into account multiscale behavior of the solution and to derive an asymptotically stable and accurate scheme, we propose the following splitting of the Navier-Stokes equations into a linear \mathcal{L} and a nonlinear \mathcal{N} part, see also [2] and the references therein. To this end let us rewrite (1) in the following compact form. Let $\mathbf{w} = (\rho', \rho \mathbf{u}, \rho \theta')^T$, $\mathbf{F}(\mathbf{w}) = (\rho \mathbf{u}, \rho \mathbf{u} \otimes \mathbf{u} + p' \text{Id}, \rho \theta \mathbf{u})^T$, $\mathbf{D}(\mathbf{w}) = (0, \nabla \cdot (\rho \mu_m (\nabla \mathbf{u} + (\nabla \mathbf{u})^T)), \nabla \cdot (\rho \mu_h \nabla \theta))^T$ and $\mathbf{S}(\mathbf{w}) = (0, -\rho' g \mathbf{e}_3, S_\theta)^T$, then (1) can be equivalently written as

$$\frac{\partial \mathbf{w}}{\partial t} = -\nabla \cdot \mathbf{F}(\mathbf{w}) + \mathbf{D}(\mathbf{w}) + \mathbf{S}(\mathbf{w}) \equiv \mathcal{L}(\mathbf{w}) + \mathcal{N}(\mathbf{w}). \quad (3)$$

We would like to point out that the choice of the linear and nonlinear operators, \mathcal{L} and \mathcal{N} , respectively, is crucial. Indeed, we choose \mathcal{L} to model linear acoustic and gravitational waves as well as a part of viscous fluxes, whereas the operator \mathcal{N} describes resulting nonlinear advective/convective and the remaining viscous effects. Analogously, to split the diffusive terms into linear and nonlinear terms in \mathbf{w} , we set $\mathbf{D} = \mathbf{D}_L + \mathbf{D}_N$ with

$$\begin{aligned} \mathbf{D}_L &= (0, \mu_m (\Delta(\rho \mathbf{u}) + \Delta(\rho \mathbf{u}^T)), \mu_h \Delta(\rho \theta)')^T, \\ \mathbf{D}_N &= (0, -\mu_m ((\mathbf{u} + \mathbf{u}^T) \Delta \rho + \nabla \rho \cdot (\nabla \mathbf{u} + \nabla \mathbf{u}^T)), \mu_h (\Delta(\overline{\rho \theta}) - \theta \Delta \rho - \nabla \rho \cdot \nabla \theta))^T. \end{aligned}$$

Analogously as in [2] we then set

$$\mathcal{L}(\mathbf{w}) \equiv -\nabla \cdot \mathcal{F}_L(\mathbf{w}) + \mathbf{S}_L(\mathbf{w}) + \mathbf{D}_L(\mathbf{w}) := -\nabla \cdot \begin{pmatrix} \rho \mathbf{u} \\ p' \text{Id} \\ \theta \rho \mathbf{u} \end{pmatrix} + \begin{pmatrix} 0 \\ -\rho' g \mathbf{e}_3 \\ 0 \end{pmatrix} + \mathbf{D}_L(\mathbf{w})$$

with the linearized pressure $p' = \gamma_m \frac{\bar{p}(\rho\theta)'}{\bar{\rho}\bar{\theta}} \left(\frac{R\bar{\rho}\bar{\theta}}{p_0} \right)^{\gamma_m - \gamma}$, where $\gamma = 1.4$ is the adiabatic constant, and

$$\mathcal{N}(\mathbf{w}) \equiv -\nabla \cdot \mathcal{F}_N(\mathbf{w}) + \mathbf{S}_N(\mathbf{w}) + \mathbf{D}_N(\mathbf{w}) := -\nabla \cdot \begin{pmatrix} 0 \\ \rho \mathbf{u} \otimes \mathbf{u} \\ \theta' \rho \mathbf{u} \end{pmatrix} + \begin{pmatrix} 0 \\ 0 \\ S_\theta \end{pmatrix} + \mathbf{D}_N(\mathbf{w}).$$

Consequently, we discretize the Navier-Stokes equations by the IMEX scheme in time and approximate the linear stiff system at a new time level t_{n+1} and the nonlinear system at the old time level t_n . This yields the first order IMEX scheme. In order to increase the accuracy, the second order IMEX schemes can be applied, see, e.g., [1, 3, 2]. In our recent papers [1, 3] we have studied several second order IMEX schemes with respect to their asymptotic preserving properties. Here we confine ourselves with the second order globally stiffly accurate ARS(2,2,2) scheme

$$\begin{aligned} \mathbf{w}^{n+\frac{1}{2}} &= \mathbf{w}^n + \alpha \Delta t \left(\mathcal{L} \left(\mathbf{w}^{n+\frac{1}{2}} \right) + \mathcal{N} \left(\mathbf{w}^n \right) \right), \\ \mathbf{w}^{n+1} &= \mathbf{w}^n + \Delta t \left(\delta \mathcal{N} \left(\mathbf{w}^n \right) + (1 - \delta) \mathcal{N} \left(\mathbf{w}^{n+\frac{1}{2}} \right) \right) \\ &\quad + \Delta t \left(\alpha \mathcal{L} \left(\mathbf{w}^{n+1} \right) + (1 - \alpha) \mathcal{L} \left(\mathbf{w}^{n+\frac{1}{2}} \right) \right), \end{aligned} \quad (4)$$

where $\alpha = 1 - \frac{1}{\sqrt{2}}$, $\delta = 1 - \frac{1}{2\alpha}$ and $\Delta t = t_{n+1} - t_n$.

Spatial discretization is realized by the finite volume scheme. In particular having a regular rectangular grid we approximate the corresponding divergence operators by applying the Gauss theorem and the numerical flux functions in order to approximate fluxes along the cell interfaces. Let us denote the finite difference in the x_1 -direction at the mesh cell $\Omega_{i,j,m} \equiv [x_i - \Delta x_1/2, x_i + \Delta x_1/2] \times [y_j - \Delta x_2/2, y_j + \Delta x_2/2] \times [z_m - \Delta x_3/2, z_m + \Delta x_3/2]$ by $\delta_{x_1} f_{i,j,m} \equiv f_{i+1/2,j,m} - f_{i-1/2,j,m}$; an analogous notation holds in the x_2 and x_3 direction. The finite volume discretization of the operators \mathcal{L} and \mathcal{N} yields

$$\begin{aligned} \mathcal{L}(\mathbf{w}^\ell)_{i,j,m} &= - \sum_{k=1}^3 \frac{1}{\Delta x_k} \delta_{x_k} \mathcal{F}_L^*(\mathbf{w}^\ell)_{i,j,m} + \mathbf{S}(\mathbf{w}^\ell)_{i,j,m} + \mathcal{D}_L(\mathbf{w}^\ell)_{i,j,m}, \quad \ell = n+1, \\ \mathcal{N}(\mathbf{w}^\ell)_{i,j,m} &= - \sum_{k=1}^3 \frac{1}{\Delta x_k} \delta_{x_k} \mathcal{F}_N^*(\mathbf{w}^\ell)_{i,j,m} + \mathcal{D}_N(\mathbf{w}^\ell)_{i,j,m}, \quad \ell = n, n-1. \end{aligned}$$

Here $\mathcal{D}_L(\mathbf{w}^\ell)$ and $\mathcal{D}_N(\mathbf{w}^\ell)$ are the second order central difference approximations of the operators $\mathbf{D}_L(\mathbf{w}^\ell)$ and $\mathbf{D}_N(\mathbf{w}^\ell)$, respectively. For the numerical fluxes on cell interfaces, i.e. $\mathcal{F}_L^*(\mathbf{w}^\ell)$ and $\mathcal{F}_N^*(\mathbf{w}^\ell)$, we apply the central difference flux in the linear subsystem \mathcal{L} and the Rusanov numerical flux in the nonlinear subsystem \mathcal{N} . To keep the finite volume approximation of the explicit advection part stable we control the time step by the Courant-Friedrichs-Lewy stability condition

$$CFL_u \equiv \max_{k=1,2,3} \max_{i,j,m} |(u_k)_{i,j,m}| \frac{\Delta t}{\Delta x_k} < 1.$$

2.2 IMEX finite volume scheme for the cloud dynamics model

Similar to the IMEX finite volume discretization of the compressible Navier-Stokes equations in Subsection 2.1, we approximate the advection-diffusion-reaction system (2) by the finite volume method in space and by the second order IMEX scheme in time.

First, we rewrite the system (2) in the following compact form. Let $\mathbf{w}_q = (\rho q_v, \rho q_c, \rho q_r)^T$, $\mathbf{F}_q(\mathbf{w}_q) = (\rho q_v \mathbf{u}, \rho q_c \mathbf{u}, \rho q_r \mathbf{u} - \rho v_q \mathbf{e}_3 q_r)^T$, $\mathbf{D}_q(\mathbf{w}_q) = \nabla \cdot (\rho \mu_h \nabla q_v, \rho \mu_h \nabla q_c, \rho \mu_h \nabla q_r)^T$ and $\mathbf{S}_q(\mathbf{w}_q) = (-C + E, C - A_1 - A_2, A_1 + A_2 - E)^T$, then (2) can be equivalently written as

$$\frac{\partial \mathbf{w}_q}{\partial t} = -\nabla \cdot \mathbf{F}_q(\mathbf{w}_q) + \mathbf{D}_q(\mathbf{w}_q) + \mathbf{S}_q(\mathbf{w}_q). \quad (5)$$

Realizing that $\mu_h \nabla \cdot (\rho \nabla q_x) = \mu_h \Delta (\rho q_x) - \mu_h q_x \Delta \rho - \mu_h \nabla \rho \cdot \nabla q_x$ for any $x \in \{c, v, r\}$ we can split \mathbf{D}_q into

$$\begin{aligned} \mathbf{D}_q^{\text{impl}} &= \mu_h (\Delta (\rho q_v), \Delta (\rho q_c), \Delta (\rho q_r))^T, \\ \mathbf{D}_q^{\text{expl}} &= -\mu_h (q_v \Delta \rho + \nabla \rho \cdot \nabla q_v, q_c \Delta \rho + \nabla \rho \cdot \nabla q_c, q_r \Delta \rho + \nabla \rho \cdot \nabla q_r)^T. \end{aligned}$$

Then, equation (5) can be rewritten as

$$\frac{\partial \mathbf{w}_q}{\partial t} = \mathbf{I}_q(\mathbf{w}_q) + \mathbf{E}_q(\mathbf{w}_q), \quad (6)$$

where $\mathbf{I}_q(\mathbf{w}_q) = \mathbf{D}_q^{\text{impl}}(\mathbf{w}_q)$ and $\mathbf{E}_q(\mathbf{w}_q) = -\nabla \cdot \mathbf{F}_q(\mathbf{w}_q) + \mathbf{D}_q^{\text{expl}}(\mathbf{w}_q) + \mathbf{S}_q(\mathbf{w}_q)$.

Let us point out that the coupled system (1), (2) has a multiscale character, since it combines fast microscopic cloud dynamics with the slower macroscopic fluid flow. Therefore, we choose the time step for the cloud dynamics $\Delta t_{\text{cloud}} = \frac{\Delta t}{\text{const.}}$ for a sufficiently big constant. Time discretization of the cloud dynamics is realized by the second order IMEX ARS(2,2,2) scheme (4), whereas the diffusive terms $\mathbf{I}_q(\mathbf{w}_q)$ are approximated implicitly at a new micro-time level t_{s+1} and the remaining terms $\mathbf{E}_q(\mathbf{w}_q)$ explicitly at the old time level t_s .

The spatial discretization is done by the finite volume scheme. With the same notation as in Subsection 2.1 the discretizations of the operators \mathbf{I}_q and \mathbf{E}_q yield

$$\begin{aligned} \mathbf{I}_q(\mathbf{w}_q^\ell)_{i,j,m} &= \mathcal{D}_q^{\text{impl}}(\mathbf{w}_q^\ell)_{i,j,m}, \quad \ell = s+1, \\ \mathbf{E}_q(\mathbf{w}_q^\ell)_{i,j,m} &= -\sum_{k=1}^3 \frac{1}{\Delta x_k} \delta_{x_k} \mathbf{F}_q^*(\mathbf{w}_q^\ell)_{i,j,m} + \mathcal{D}_q^{\text{expl}}(\mathbf{w}_q^\ell)_{i,j,m} + \mathbf{S}_q(\mathbf{w}_q^\ell)_{i,j,m}, \quad \ell = s, s-1, \end{aligned}$$

where $\mathcal{D}_q^{\text{expl}}(\mathbf{w}_q^\ell)$ is a second order central difference approximation of $\mathbf{D}_q^{\text{expl}}(\mathbf{w}_q^\ell)$; analogous notation holds for $\mathcal{D}_q^{\text{impl}}(\mathbf{w}_q^\ell)$. For the numerical fluxes on the cell interfaces $\delta_{x_k} \mathbf{F}_q^*(\mathbf{w}_q^\ell)$ we apply the Lax-Friedrichs numerical flux.

3 Numerical test

In this test we simulate free convection of a smooth warm air bubble as proposed in [5], see also [8]. A warm air bubble that is surrounded by cold air is placed on the bottom of the domain. Since the density of the warm air is lower than the surrounding air, the bubble rises up due to the buoyancy force. The experiment was simulated on a two-dimensional ($x_1 - x_3$ plane) domain $\Omega = [0, 20.0] \times [0, 10.0]$ [km^2].

The initial conditions for the Navier-Stokes equations are chosen as

$$\begin{aligned} \rho' &= \frac{p_0}{R} \pi_e^{\frac{1}{\gamma-1}} \left(\frac{1}{\theta} - \frac{1}{\bar{\theta}} \right) = -\bar{\rho} \frac{\theta'}{\bar{\theta}}, \quad \pi_e = 1 - \frac{g x_3}{c_p \bar{\theta}}, \quad \bar{\rho} = \frac{p_0}{R \bar{\theta}} \pi_e^{\frac{1}{\gamma-1}}, \\ \mathbf{u} &= 0, \\ \theta' &= \begin{cases} 0, & r > r_c, \\ 2 \cos^2 \left(\frac{\pi r}{2} \right), & r \leq r_c, \end{cases} \end{aligned}$$

where $\bar{\theta} = 300$ [K], $r = \|(x_1, x_3)^T - (10.0, 2.0)^T\|_2$ [km], $r_c = 2.0$ [km], $p_0 = \bar{p} = 10^5$ [Pa] and $(x_1, x_3)^T \in \Omega$. For the cloud model the initial conditions are

$$q_v = \min(q_* f(x_3), 0.014), \quad q_c = 0, \quad q_r = 0,$$

where f is the relative humidity and given by

$$f(x_3) = 1 - \frac{3}{4} \left(\frac{x_3}{x_{tr}} \right)^{5/4}, \quad x_{tr} = 12$$
 [km].

We apply the no-flux boundary conditions $\mathbf{u} \cdot \mathbf{n} = 0$, $\nabla \rho' \cdot \mathbf{n} = 0$, $\nabla(\rho \theta)' \cdot \mathbf{n} = 0$.

In Fig. 1 the time evolution of a moist air bubble, obtained by the ARS(2,2,2) finite volume approximation, is shown. The results for the potential temperature as well as for the vertical velocity are quite similar to the ones by Bryan and Fritsch proposed in [5] which confirms the reliability of our numerical model.

Acknowledgements The research leading to these results has been done within the subproject A2 of the Transregional Collaborative Research Center SFB/TRR 165 ‘‘Waves to Weather’’ funded by the German Science Foundation (DFG). The authors acknowledge the support of the Data Center ZDV in Mainz for providing computation time on MOGON cluster.

References

1. Bispen, G., Arun, K.R., Lukáčová-Medvidová, M., Noelle, S.: IMEX large time step finite volume methods for low Froude number shallow water flows. *Comm. Comput. Phys.* **16**, 307–347 (2014)
2. Bispen, G., Lukáčová-Medvidová, M., Yelash, L.: IMEX finite volume evolution Galerkin schemes for three-dimensional weakly compressible flows. In: A. Handlovičová (ed.) *Algo-*

- ritmy 2016, pp. 62–73 (2016)
3. Bispen, G., Lukáčová-Medvidová, M., Yelash, L.: Asymptotic preserving IMEX finite volume schemes for low Mach number Euler equations with gravitation. *J. Comput. Phys.* (2017)
 4. Brdar, S., Dedner, A., Klöfkom R. Kränkel, R., Kröner, D.: Simulation of geophysical problems with DUNE-FEM. In: E. Krause (ed.) *Computational Sci., & High Performance Computing IV*, NNFM 115, pp. 93–106. Springer (2011)
 5. Bryan, G., Fritsch, J.M.: A benchmark simulation for moist nonhydrostatic numerical models. *Monthly weakly review* **130**, 2917–2928 (2002)
 6. Khain, A.P., Beheng, K.D., Heymsfield, A., Korolev, A., Krichak, S.O., Levin, Z., Pinsky, M., Phillips, V., Prabhakaran, T., Teller, A., van den Heever, S.C., Yano, J.I.: Representation of microphysical processes in cloud-resolving models: Spectral (bin) microphysics versus bulk parameterization. *Reviews of Geophysics* **53**, 247–322 (2015)
 7. Lamb, D., Verlinde, J.: *Physics and chemistry of clouds*. Cambridge University Press (2011)
 8. Schuster, D., Brdar, S., Baldauf, M., Dedner, A., Klöfkom, R., Kröner, D.: On discontinuous Galerkin approach for atmospheric flow in the mesoscale with and without moisture. *Meteorologische Zeitschrift* **23**(4), 449–464 (2011)
 9. Wacker, U.: Structural stability in cloud physics using parameterized microphysics. In: *Beitr. Phys. Atmosph.* 65, pp. 231–242 (1992)

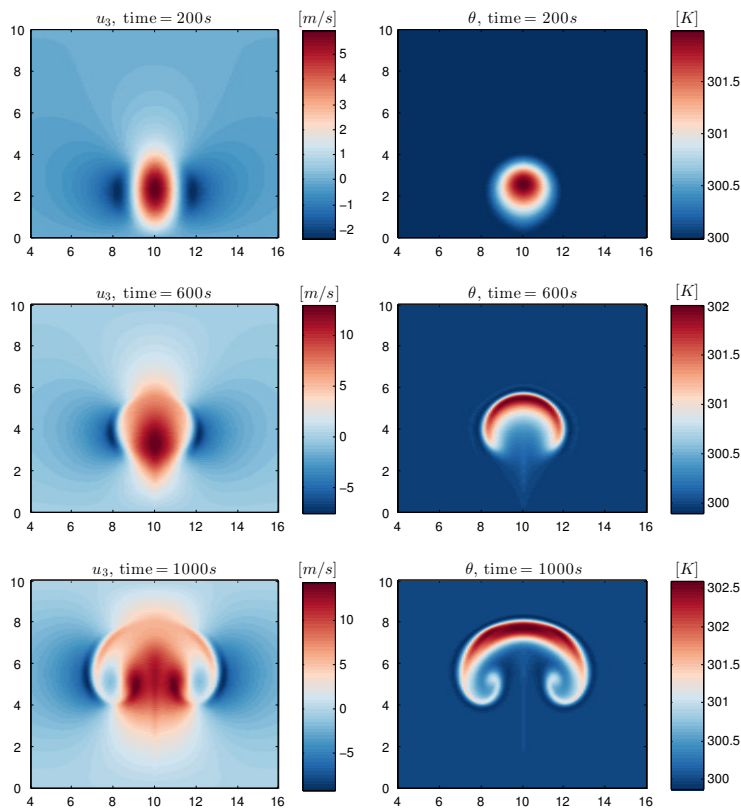


Fig. 1 Rising moist air bubble test computed by the IMEX ARS(2,2,2) finite volume scheme; $\mu_h = 10^{-2}$, $\mu_m = 10^{-3}$, $CFL_u = 0.4$, the mesh resolution $\Delta x_1 = 100 [m]$ and $\Delta x_3 = 50 [m]$. The colors correspond to the vertical velocity u_3 (left column) and the moist potential temperature θ (right column).